

Effects of surface and crystalline defects on reverse characteristics of 4H-SiC JBS diodes

Takashi Katsuno¹, Yukihiro Watanabe¹, Hirokazu Fujiwara², Masaki Konishi², Takeo Yamamoto³ and Takeshi Endo³

¹Toyota Central R&D Laboratories Inc.

41-1, Yokomichi, Nagakute, Nagakute-cho, Aichi, 480-1192, Japan

Phone: +81-561-71-7021 Fax: +81-561-63-6927 E-mail: e1417@mosk.tytlabs.co.jp

²TOYOTA MOTOR CORPORATION

543, Kirigahora, Nishihiro-cho, Toyota, Aichi, 470-0309, Japan

³Research Laboratories, DENSO CORPORATION

500-1, Minamiyama, Komenoki-cho, Nisshin-shi, Aichi, 470-0111, Japan

1. Introduction

Silicon carbide (SiC) is suitable material for the use of the next generation power devices, because it has the excellent thermal, mechanical and electrical properties compared to silicon (Si) due to the high thermal conductivity, high band gap and high electron mobility, etc.. Recently, large area 4H-SiC wafers with high quality are released from several companies [1, 2], and SiC devices have been developed by many groups [3-6]. However, the reverse characteristics of many SiC diodes prepared on a SiC wafer are usually dispersed, ranging from low blocking voltage to high leakage current. It is needed to solve the problem immediately.

It is already reported that some surface defects (micropipe, particle, and triangle defect etc.) have influences on the reverse characteristics of SiC diodes [7-10]. However, the results still have unclear. Because SiC wafers still content some surface and crystalline defects, and it is difficult to decide the effects by the surface and crystalline defects on the reverse characteristics. In order to clarify the relation between the dispersed reverse characteristics of SiC diodes and the surface defects, we investigated the surface defects on SiC diodes by the optical microscope and scanning electron microscope (SEM). Furthermore, the effects of crystalline defects were also investigated.

2. Experiment

A commercial 4^o off n-type 4H-SiC wafer with 13 μm thick epitaxial layer doped with $5.0 \times 10^{15} \text{ cm}^{-3}$ of nitrogen was used to fabricate Junction Barrier Schottky (JBS) diode. The width of striped p layer in the active area is 1 μm , and the space between the striped p layer is 2 μm . Mo was used as a Schottky electrode, and the electrode diameter was 3.9 mm ϕ . The reverse characteristics of 4H-SiC diodes (128 samples) were dispersed, and divided in 3 modes as shown in Fig. 1. A mode is the low blocking voltage samples. B mode is high leakage current samples, and C mode is low leakage current samples. Sample numbers of A to C modes counted from Fig. 1 are 39, 16 and 73, respectively, as shown in Table 1. 10, 6 and 8 analyzed samples were randomly selected from A to C modes, respectively. In

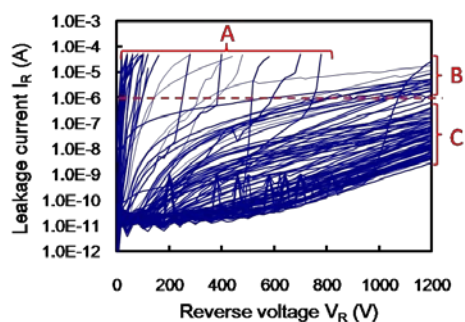


Fig. 1. Reverse characteristics of 4H-SiC diode.

Table 1. The number of 4H-SiC JBS diode in the classification of the reverse characteristics.

	Classification of the reverse properties	Number of sample	Number of analysis sample
A mode	Low blocking voltage	39	10
B mode	High leakage current	16	6
C mode	Low leakage current	73	8
Total	-	128	24

order to exist the surface defects on the SiC surfaces, the electrodes were removed by the chemical wet etching after the measurements of reverse characteristics. Then, the SiC surfaces were observed by optical microscope and SEM. After the observation of SiC surfaces, we focused on the crystalline defects [e.g. threading screw dislocation (TSD) and threading edge dislocation (TED)], transformed to the etch pits produced by molten KOH etching. The molten KOH etching temperature and the time were 500 $^{\circ}\text{C}$ and 10 min., respectively.

3. Results and Discussion

<3.1> In A mode of low blocking voltage samples, the micropipes and the particle were observed on the SiC surfaces as shown in Fig.2. The sizes of micropipe and the particle were about 1 and 22 μm , respectively. Si and C as the elements were detected from the particle, analyzed by Energy Dispersive X-ray spectroscopy (EDX). It is expected that the particles would come from the wall during the epitaxial growth. It is well known that the

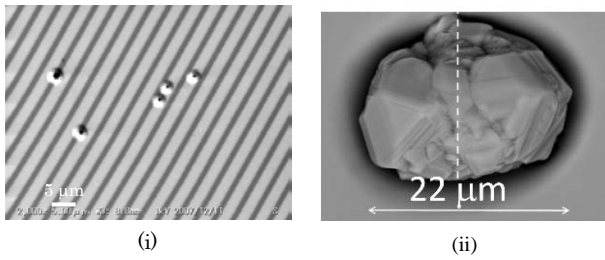


Fig. 2. SEM images of surface defects in A mode.
(i) Micropipe, (ii) Particle.

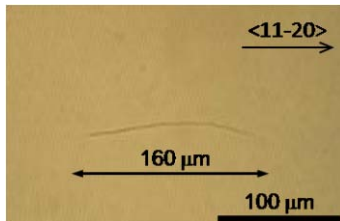


Fig. 3. Optical image of carrot-like defect observed in B mode.

micropipe is caused to low blocking voltage on the reverse characteristics [7-10], which is the same result.

<3.2> In B mode of high leakage samples, the straight-shaped defect was observed by the optical microscope as shown in Fig. 3. This defect seems to be carrot-like defect. The defect exists toward to <11-20> direction and the length is about 160 μm . In all 6 samples of B mode, the carrot-like defects were observed and the other surface defects such as the micropipe and the particles were not observed. Thus, the carrot-like defect is caused to the increase of leakage current.

<3.3> In C mode of low leakage current samples, there is no surface defects on the SiC surfaces observed by the optical microscope in all 8 samples. We focused on the crystalline defects (TSDs and TEDs) instead of the surface defects. Fig. 4 shows the optical image of etch pits for TSDs and TEDs, produced by molten KOH etching. The numbers of etch pits in the active area were counted, and plotted the relation between etch pit density (EPD) and leakage currents obtained at 1200 V as shown in Fig. 5. The leakage current increased at an almost constant rate increasing with EPD, which values are from 10^3 to 10^5 cm^{-2} . From this tendency, a etch pit of threading dislocation is caused to the increase of leakage current about 10^{-9} A.

4. Conclusions

In order to clarify the relation between the dispersed reverse characteristics of SiC diodes and the defects, we investigated the surfaces and crystalline defects of SiC diodes. The good relations between the reverse characteristics of 4H-SiC and the surface defects were obtained. Furthermore, the good relationship between the leakage current and EPD were also obtained, affecting that a etch pit of threading dislocation was caused to the increase of leakage current about 10^{-9} A in case of this JBS structure. Micropipe and particle were caused to the low

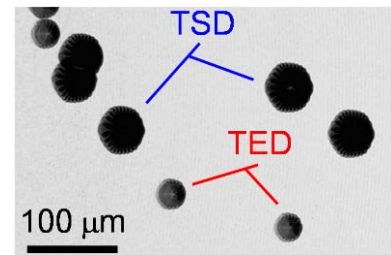


Fig. 4. Optical image of etch pits for TSD and TED.

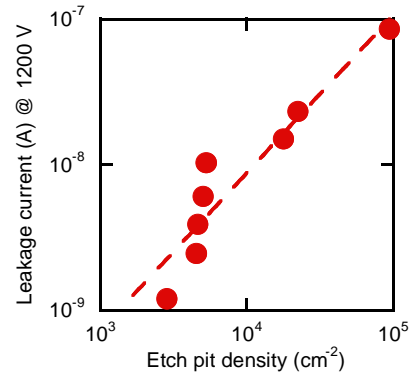


Fig. 5. Relationship between leakage current and etch pit density in C mode.

blocking voltage, and carrot-like defect was caused to high leakage current. The dispersion could be seen in C mode, but there are no surface defects. The leakage current depended on the EPD of threading dislocations.

References

- [1] E. Berkman, R. T. Leonard, M. J. Paisley, Y. Khlebnikov, M. J. O'Loughlin, A. A. Burk, A. R. Powell, D. P. Malta, E. Deyneka, M. F. Brady, I. Khlebnikov, V. F. Tsvetkov, H. McD. Hobgood, J. Sumakeris, C. Basceri, V. Balakrishna, C. H. Carter, Jr. and C. Balkas, *Materials Science Forum*, **615-617** (2009) 3.
- [2] B. Thomas, C. Hecht and B. Kallinger, *Materials Science Forum*, **615-617** (2009) 77.
- [3] Q. Wahab, A. Ellison, A. Henry, E. Janzen, C. Hallin, J. Di Persio and R. Martinez, *Appl. Phys. Lett.*, **76** (2000) 2725.
- [4] M. Ruff, H. Mitlehner and R. Helbig, *IEEE Transaction on Electron Devices*, **41** (1994) 1040.
- [5] T. Kimoto, N. Miyamoto and H. Matsunami, *IEEE Transaction on Electron Devices*, **46** (1999) 471.
- [6] L. Chen, O. J. Guy, D. Doneddu, S. G. J. Batcup, S. P. Wilks, P. A. Mawby, T. Bouchet and F. A. Torregrosa, *Microelectronics Reliability*, **46** (2006) 637.
- [8] K.-Y. Lee and M. A. Capano, *J. Electronic Materials*, **36** (2007) 272.
- [9] H. Fujiwara, T. Kimoto, T. Tojo and H. Matsunami, *Appl. Phys. Lett.*, **87** (2005) 1-1.
- [10] S. Tumakha, D. J. Ewing, L. M. Porter, Q. Wahab, X. Ma, T. S. Sudharshan and L. J. Brillson, *Appl. Phys. Lett.*, **87** (2005) 242106-1.